SLURRY EROSION RESISTANCE OF LASER CLAD Fe–Cr–B–Si COATINGS

W. H. Jiang and R. Kovacevic

The slurry erosion behaviour of laser clad Fe–Cr–B–Si alloy coatings was investigated at impact angles from 30° to 90° with an increment of 15°, and compared with the slurry erosion behaviour of two laser clad carbide coatings and a non-coated substrate made of AISI 4140 steel. The Fe–Cr–B–Si alloy coatings had slurry erosion resistance. Their overall slurry erosion resistance at impact angles from 30° to 90° was higher than both the carbide coatings and steel. The erosion resistance of the Fe–Cr–B–Si alloy coatings was less dependent on slurry impact angle. The Fe–Cr–B–Si alloy coatings consisted of the Fe–Cr solid solution matrix and the second phase Fe_2B. The laser beam traverse rate had little effect on the erosion resistance and microstructures of the coatings. The liquid nitrogen cooling of the substrate resulted in a structural refinement of the deposited coating and increased the erosion resistance substantially. SE/S308

The authors are in the Research Center for Advanced Manufacturing, School of Engineering, Southern Methodist University, 1500 International Parkway, Suite #100, Richardson, TX 75081, USA (kovacevi@engr.smu.edu). *Received 5 May 2004; accepted 7 July 2004.*

***Keywords**: Laser cladding, Coating, Slurry erosion, Wear, Surface modification, Boride, Tungsten carbide, Chromium carbide, Liquid nitrogen cooling, Microstructure, Hardness, Steel, Impact, Composite coating, Structural refinement*

INTRODUCTION

Slurry erosion happens extensively in mining, metallurgy and crude oil drilling. During extraction and transportation of slurry, the surfaces of pipes and pumps are damaged severely by the high velocity impact of a fluid flow containing hard particles. Materials with improved wear resistance to slurry erosion are in increasing demand from the industries.

The slurry erosion process is relatively complex. The factors affecting erosion can be divided into three classes:

(i) the properties of target materials
(ii) the properties of impingement particles
(iii) the erosion conditions.[1]

Much attention has been paid to studying the slurry erosion of various materials.[2–9] Despite the fact that some relationships between the properties of some materials and their erosion resistance have been recognised,[6] materials demonstrate great differences in erosion resistance under different conditions. Therefore, wear resistant materials need to be identified in simulated service conditions.

The widely used Coriolis slurry erosion tester is designed to simulate particle sliding or a low angle impact condition.[10,11] Because a fluid flow is almost parallel to the surfaces of the components, this tester is suitable for examining the erosion behaviour of materials of a pipe wall. Yet, some critical components in a pumping system suffer owing to the strong impact of a fluid flow containing hard sand particles at angles from 0° to 90°. Therefore, a slurry jet erosion test at various impact angles is necessary.

It has been realised that producing a hard coating on the surfaces of components is an effective route to protecting substrates from slurry erosion.[2,5,7–9] Owing to their high hardness and availability, carbides,[8,9,11] especially refractory metal carbides, have been used commercially as hard coating materials. However, the erosion resistance of carbide coatings at high impact angles is not as effective as at low impact angles. Erosion resistant coatings that can respond to a wide range of impact angles are needed.

The present work investigates the slurry erosion resistance of laser clad Fe–Cr–B–Si coatings with respect to two types of commercially available carbide coatings, Metco 430 (Cr_2C_3 + Ni20Cr, −53 to +11 μm) and AMDRY 302 (W_2C/WC + 12%Co (fused), −125 to +45 μm), and with respect to AISI 4140 steel.

EXPERIMENTAL PROCEDURE

The precursor powder of an Fe–Cr–B–Si alloy used in the present work is a commercial product (LMC-M) with a nominal constitution: Fe–43·0–46·0Cr–5·6–6·2B–1·75–2·25 Si–<0·17 C–<0·02S (wt-%), which is produced by gas atomisation. X-ray diffraction (XRD) analysis demonstrated that the precursor powder consists of an Fe–Cr solid solution and an Fe_2B phase. A 4140 steel plate with a nominal composition Fe–0·38–0·43C–0·8–1·1Cr–0·75–1Mn–0·15–0·25Mo–0·15–0·35Si–<0·035P–<0·04S (wt-%) was used as a substrate.

Coating layers were achieved using an Nd:YAG laser with maximum power 1 kW in a continuous wave form. The laser beam power used in the experiments was in the range 0·3–0·5 kW, with a spot diameter of 1 mm. In order to examine the effect of a laser beam traverse rate on erosion resistance, the rates of 5·08 mm s^{-1}, 7·62 mm s^{-1} and 10·16 mm s^{-1} were chosen. A 40% overlap of successive melting tracks was taken. A powder feeding system was used for the direct injection of powders with an argon flow as the powder carrier. The powder was injected through four nozzles 1 mm in diameter at a rate of 5–10 g min^{-1}. Substrate samples (25·4 mm, 25·4 mm) were coated with a single layer 0·8 mm thick.

 DOI 10.1179/174329404X7135

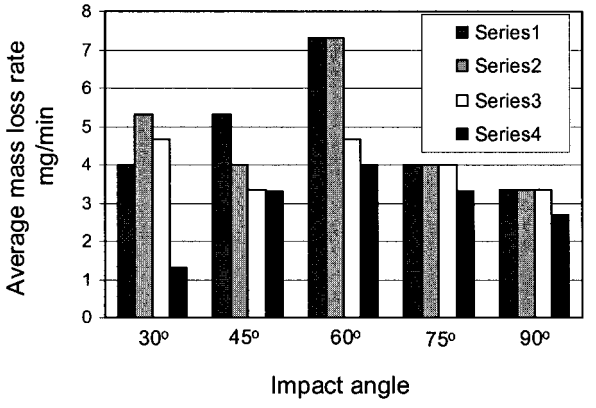

laser beam traverse rates: *1* 10·16 mm s^{-1}; *2* 7·62 mm s^{-1}; *3* 5·08 mm s^{-1}; *4* 10·62 mm s^{-1} (with liquid N_2 cooling)

1 *Slurry erosion rates of Fe–Cr–B–Si alloy coatings at various impact angles*

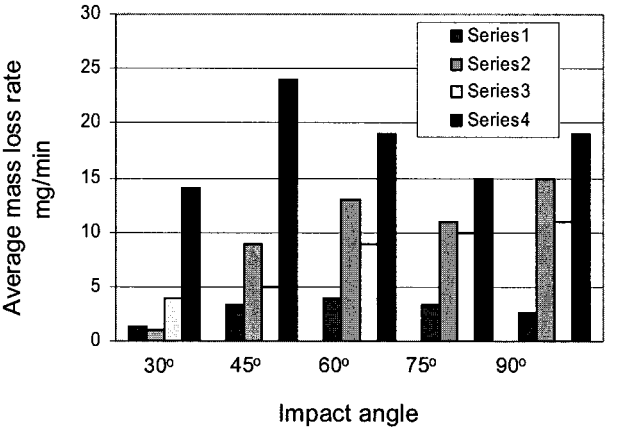

1 Fe–Cr–Si–B coating (with liquid N_2 cooling); *2* tungsten carbide coating; *3* chromium carbide coating; *4* AISI 4140 steel

2 *Comparison of erosion rates of Fe–Cr–B–Si alloy coatings produced by laser cladding at laser beam traverse rate of 10·16 mm s^{-1} with liquid nitrogen cooling with those of carbide coatings and AISI 4140 steel*

To increase the cooling rate of the deposited layers further, a cooling box with liquid nitrogen flowing continuously through it was placed just below a substrate. When the temperature of the substrate drops below −140°C, the laser deposition process was initiated at the beam scanning speed of 10·16 mm s^{-1}.

The microstructures of the coated layers were observed using optical microscopy and SEM. Microhardness measurements were conducted through the thickness of a coated layer using a hardness tester with a load of 100 g.

The slurry jet erosion tester used for this experiment was similar to the Coriolis erosion tester, except that the slurry jet tester has the capability to change the angle of the slurry impact. The slurry erosion tester utilises a centrifugal acceleration in a revolving rotor to push slurry rapidly onto a sample surface such that the solid particles were forced against the surface, producing wear during impact. Duplicate samples were used in each test. The samples were placed 30 mm from a nozzle, which allows for the possibility of changing the impact angle with respect to flow. Impact angles were changed from 30° to 90° with an increment of 15°. The rotational speed used in all tests was 875 rev min^{-1}, giving an impact speed of 25 m s^{-1} onto the sample surfaces. The slurry was made of 12 wt-% spherical silica sand (SiO_2) in water. The hardness of the silica was taken to be ~750 HV.[12] Its size was between 425 m and 850 m. Each erosion test lasted 15 min.

The specimen weight loss was measured, and an erosion rate was calculated. The eroded surfaces and subsurfaces were observed using SEM.

RESULTS AND DISCUSSION

The slurry erosion resistance of the Fe–Cr–B–Si alloy coatings produced at the laser beam traverse rates of 5·08 mm s^{-1}, 7·62 mm s^{-1} and 10·16 mm s^{-1} and under liquid nitrogen cooling was examined. Figure 1 shows their slurry erosion rates at various impact angles. It can be seen that a laser beam traverse rate has no influence on the erosion rate of the coatings at higher impact angles (75° and 90°). But, at lower impact angles, except 30°, the erosion rates decrease with decreasing laser beam traverse rate. Furthermore, the coating with liquid nitrogen cooling demonstrates the best erosion resistance of the Fe–Cr–B–Si alloy coatings.

The erosion resistance of the Fe–Cr–B–Si alloy coating with liquid nitrogen cooling was compared with the erosion resistance of AISI 4140 steel (substrate material), laser clad chromium carbide and tungsten carbide coatings, as shown in Fig. 2. It can be seen that the Fe–Cr–B–Si alloy coating had superior erosion resistance over the steel, chromium carbide coating and tungsten carbide coating at all impact angles except 30°, where the tungsten carbide had the least erosion. The hard carbide coatings suffered the most severe erosion at normal impact, while the ductile AISI 4140 steel had the largest erosion rate at 45°. Unlike these materials, the Fe–Cr–B–Si alloy coating seemed to experience the most severe erosion at an impact angle of 60°. Compared with the ductile steel and the hard carbide coatings, the Fe–Cr–B–Si alloy coating was less dependent on the impact angle.

XRD analysis demonstrated that there are two phases in all the Fe–Cr–B–Si alloy coatings: an Fe–Cr solid solution matrix and an Fe_2B phase. Typical XRD patterns are shown in Fig. 3. The laser beam traverse rates and liquid nitrogen cooling have not changed the constituents of the coatings. It was also noted that the coatings have the same constituents as the precursor powder. This result indicates that laser melting did not modify the phase constitution. Extensive microstructural observation demonstrated that the laser beam traverse rate seems to have little effect on the microstructures of the alloy coatings. However, liquid nitrogen cooling affected the microstructures of the coated layer. The microstructures of the cross-sections of the coated layers without and with liquid nitrogen cooling are shown in Fig. 4. A large amount of Fe_2B was distributed in the Fe–Cr solid solution matrix of the coating. It can be seen that the coating cooled with liquid nitrogen has a finer microstructure. This result should be attributed to the limited growth of crystals due to rapid cooling. Microstructural examination also indicated that there was good bonding at the interfaces between the

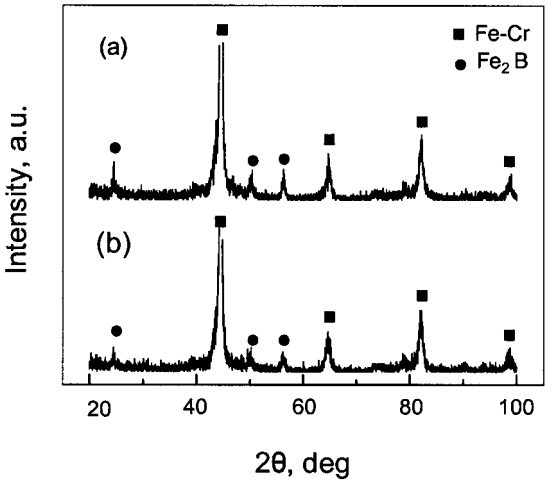

3 *XRD patterns of Fe–Cr–B–Si alloy coatings produced at laser beam traverse rate 10·16 mm s^{-1} without and with liquid nitrogen cooling*

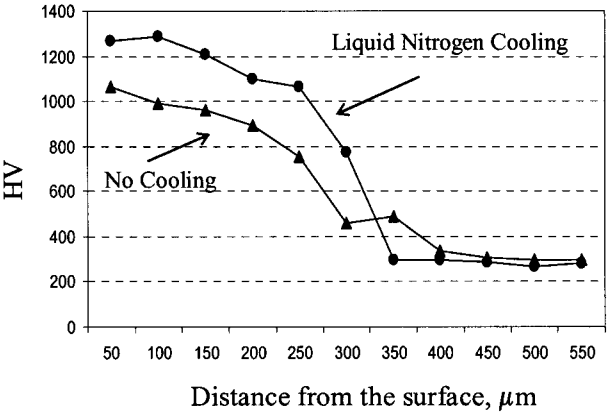

6 *Hardness profiles of Fe–Cr–B–Si alloy coatings produced at laser beam traverse rate 10·16 mm s^{-1} without and with liquid nitrogen cooling*

coatings and substrate, as shown in Fig. 5. Rapid cooling resulted in more Fe_2B at the interface zone. This result may be related to less dilution at the interface zone of the coating and the substrate when liquid nitrogen cooling was used.

The hardness profiles through the depth of the coated layers are shown in Fig. 6. The coated layers have a much higher hardness than the substrate. Within the coated layers, there was a gradual decrease in hardness from the outer surface to the substrate. Liquid nitrogen cooling increased hardness by about 20%. The coated layer cooled with liquid nitrogen has a hardness of more than 1200 HV near the outer surface, higher than that of the coating obtained without cooling by liquid nitrogen.

Erosion resulted in the formation of wear scars at the surfaces of the coated layers, which was similar to the situation in the steel, but less severe. Evidently, the centres of wear scars experienced the most severe erosion.

Figure 7 shows secondary electron images (SEI) of the eroded surface of Fe–Cr–B–Si alloy coatings without and with liquid nitrogen cooling at an impact angle of 30°. A number of ploughs can be seen on the surfaces of both coatings. This result indicates that substantial plastic deformation and micro cutting occurred at the acute impact angle. The coating with liquid nitrogen cooling experienced less erosion than the coating without cooling. This result may be

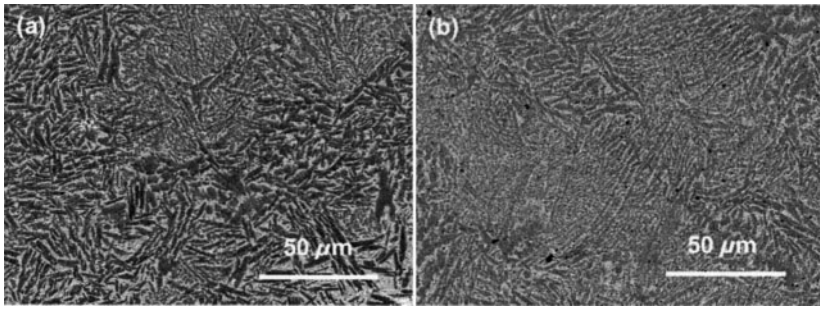

a without liquid nitrogen cooling; *b* with liquid nitrogen cooling

4 *Microstructures of Fe–Cr–B–Si alloy coatings produced at laser beam traverse rate 10·16 mm s^{-1}*

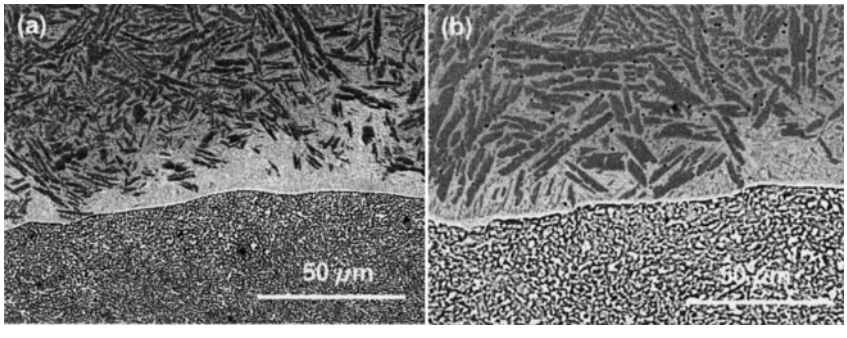

a substrate without liquid nitrogen cooling; *b* with liquid nitrogen cooling

5 *Microstructures of interface between Fe–Cr–B–Si alloy coatings produced at laser beam traverse rate 10·16 mm s^{-1}*

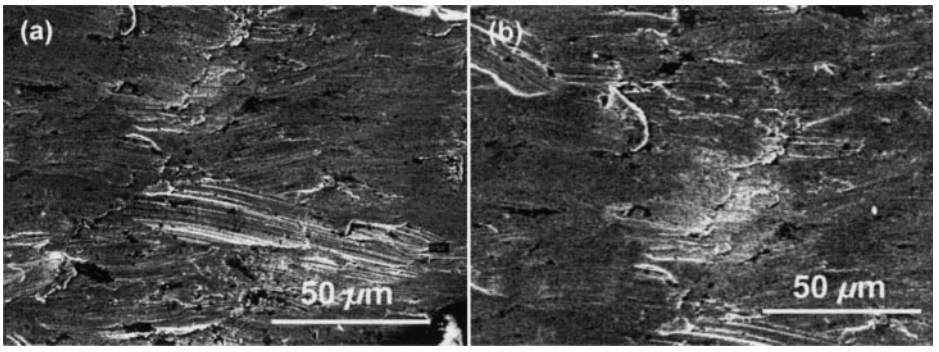

a without liquid nitrogen cooling; *b* with liquid nitrogen cooling

7 *Secondary electron images of eroded surfaces of Fe–Cr–B–Si coatings produced at laser beam traverse rate of 10·16 mm s^{-1} at impact angle 30°*

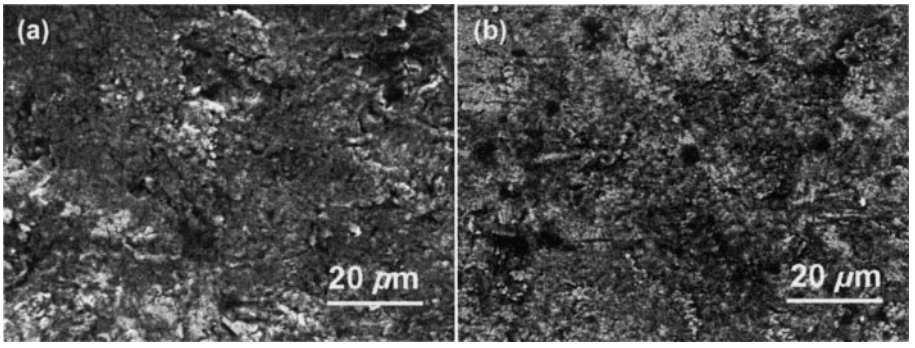

a with liquid nitrogen cooling; *b* without liquid nitrogen cooling

8 *Secondary electron images of eroded surface of Fe–Cr–B–Si coatings produced at laser beam traverse rate of 10·16 mm s^{-1} at impact angle 90°*

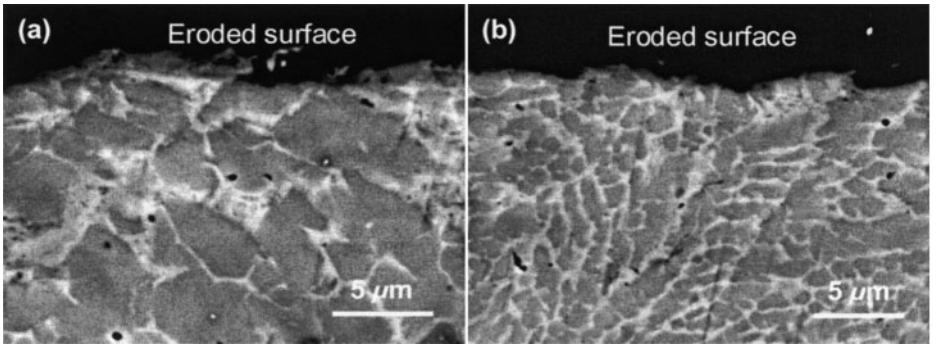

9 *Eroded subsurfaces of Fe–Cr–B–Si coatings produced at laser beam traverse rate 10·16 mm s^{-1}*

related to its higher hardness due to rapid cooling. Evidently, its erosion mechanism was the same as that of other materials at low impact angles. Micro cutting was a predominant removal mechanism of these coatings, but it was much less severe than the ductile steel in the case of erosion at an acute impact angle.[13]

Figure 8 shows the eroded surfaces of the Fe–Cr–B–Si alloy coatings without and with liquid nitrogen cooling at normal impact. It can be seen that there are some pits and a few cracks on both surfaces. The two coatings had similar eroded morphology, except that the coating with liquid nitrogen cooling was less eroded. Delamination may be the main erosion mechanism at a normal impact. A strong impact causes extensive plastic deformation, and a loss of ductility results in fracture and delamination.

The subsurface observation demonstrates that the Fe_2B grains form a load bearing structure (Fig. 9). It was found that, unlike the carbides, these borides are not a preferential path for crack propagation. Contrarily, they may act as a barrier for crack propagation. The result of that barrier was an improvement in the erosion resistance.

The effect of the impact angle on the erosion of materials is related to the mechanical properties of the materials. The erosion rates of the hard coatings increase with increasing impact angle and reach a maximum rate at an angle of 90°. Ductile materials suffer the most severe erosion at an acute angle. Such a characteristic feature is well known in dry erosion, where ductile materials usually show greater wear at low angles, while brittle materials tend to wear most at a normal impact.[7,14] However, it was reported that such trends are less clear in slurry erosion.[7]

The Fe–Cr–B–Si alloy coatings demonstrate erosion behaviour different from that of both the

hard carbide coatings and the ductile steel. It has relatively low overall erosion wear, and the minimum erosion occurs at an impact angle of 60°. Observation of the eroded surface morphologies indicates that the erosion mechanism of the Fe–Cr–B–Si alloy coating was similar to both the hard carbide coating and ductile steel. That is, the deformation wear was a predominant mechanism for normal impact, while the cutting wear becomes more prominent with decreasing impact angle. Generally speaking, the type of erosion that prevails depends on the mechanical properties of the eroded materials. For example, carbide coatings have a hardness of 1000–1200 HV, higher than that of the erodent at 720 HV.[12] Therefore, they have a higher resistance to micro cutting, which was the predominant mechanism of ductile materials for which the greatest erosion occurred at an acute angle. Conversely, the hard, brittle carbide coatings have low ductility and, consequently, they have the least wear resistance at a normal impact. The AISI 4140 steel has a hardness of only 270 HV, much lower than that of the erodent. Consequently, the steel exhibits a very low resistance to micro cutting. The different erosion behaviour of the Fe–Cr–B–Si alloy coatings without and with liquid nitrogen cooling may be attributed to the difference in hardness.

The Fe–Cr–B–Si alloy coatings without and with liquid nitrogen cooling have a better overall erosion resistance than do the carbide coatings, despite the fact that they have approximately the same hardness. It is believed that there are two reasons for this difference. One reason is that the Fe–Cr–B–Si alloy coatings may have a higher ductility and toughness, and, thus, better overall mechanical properties than the carbide coatings. The other reason is that the different microstructures could result in different erosion mechanisms. For example, the chromium carbide coating and tungsten carbide coating have roughly the same hardness, but their erosion behaviours are substantially different. In the chromium carbide coating, the high velocity impact of the slurry fractured into coarse, flake carbides causing their removal. In the tungsten carbide coating, it seems that the binder material was dug out preferentially, resulting in debonding of the carbides.[13] This result indicates that the slurry erosion mechanism is related to not only the mechanical properties but also the microstructure of the materials. Observations on the subsurface of the eroded Fe–Cr–B–Si alloy coating indicate that a very fine Fe_2B forms a load bearing structure and resists crack propagation.

SUMMARY

Using a slurry erosion tester, the slurry erosion behaviour of Fe–Cr–B–Si alloy coatings was investigated at impact angles from 30° to 90° with an increment of 15°, and compared with the slurry erosion behaviour of a chromium carbide coating, tungsten carbide coating and AISI 4140 steel. The following conclusions were obtained.

1. The Fe–Cr–B–Si alloy coatings have excellent slurry erosion resistance. Their overall slurry erosion resistance at impact angles from 30° to 90° is higher than both carbide coatings and AISI 4140 steel.
2. Unlike carbide coatings and ductile steel, the Fe–Cr–B–Si alloy coatings have an erosion resistance less dependent on the impact angle.
3. On normal impact, delamination is the erosion mechanism for the alloy coatings, while at acute impact angles, ploughing and micro cutting are the predominant erosion mechanisms.
4. The laser clad alloy coating consists of an Fe–Cr solid solution matrix and second phase Fe_2B.
5. The laser beam traverse rate has little effect on the erosion resistance and microstructures of the alloy coatings.
6. Liquid nitrogen cooling of a substrate results in a structural refinement of the deposited alloy coating and, consequently, increases the erosion resistance substantially.

ACKNOWLEDGEMENTS

The authors acknowledge the help of Mr M. Valant, Z. G. Liu and R. Dwivedi in execution of the experimental work.

REFERENCES

1. SHIGETAKA WADA and NAOYOSHI WATANABE: *J. Ceram. Soc. Jpn*, 1987, **95**, 573–578.
2. H. M. CLARK and R. B. HARTWICH: *Wear*, 2001, **248**, 147–161.
3. M. TALIA, H. LANKARANI and J. E. TALIA: *Wear*, 1999, **225–229**, 1070–1077.
4. R. DASGUPTA, B. K. PRASAD, A. K. JHA, O. P. MODI, S. DAS and A. H. YEGNESWARAN: *Wear*, 1997, **213**, 41–46.
5. H. W. HOPPEL, H. MUGHRABI, H.-G. SOCKEL, S. SCHMIDT and G. VETTER: *Wear*, 1999, **225–229**, 1088–1099.
6. H. M. CLARK and R. J. LIEWELLYN: *Wear*, 2001, **250**, 32–44.
7. H. M. HAWTHORNE, B. ARSENAULT, J. P. IMMARIGEON, J. G. LEGOUX and V. R. PARAMESWARAN: *Wear*, 1999, **225–229**, 825–834.
8. S.-P. LU, O.-Y. KWON and Y. GUO: *Wear*, 2003, **254**, 421–428.
9. D.-W. ZHANG and T. C. LEI: *Wear*, 2003, **255**, 129–133.
10. J. TUZSON: *ASME J. Fluids Eng.*, 1984, **106**, 135–140.
11. R. J. LIEWELLYN, S. K. YICK and K. F. DOLMAN: *Wear*, 2004, **256**, 592–599.
12. H. S. AVERY: 'Wear of materials', 148–157; 1977, New York, ASME.
13. W. H. JIANG and R. KOVACEVIC: 2003, unpublished work.
14. I. FINNIE: *Wear*, 1995, **186–187**, 1–10.